Title

Importance of Unimolecular HO2 Elimination in the Heterogeneous OH Reaction of Highly Oxygenated Tartaric Acid Aerosol

Journal

The Journal of Physical Chemistry A, 120(29)

ISSN

1089-5639

Authors

Cheng, Chiu Tung

Chan, Man Nin

Wilson, Kevin R

Publication Date

2016-07-28

DOI

10.1021/acs.jpca.6b05289

Peer reviewed

Importance of Unimolecular HO_2 Elimination in the Heterogeneous OH Reaction of Highly Oxygenated Tartaric Acid Aerosol

Chiu Tung Cheng [a], Man Nin Chan [a,b*], Kevin R. Wilson [c*]

[a] *Earth System Science Programme, Faculty of Science, The Chinese University of Hong Kong, Hong Kong, China*

[b] *The Institute of Environment, Energy and Sustainability, The Chinese University of Hong Kong, Hong Kong, China*

[c] *Chemical Sciences Division, Lawrence Berkeley National Laboratory, Berkeley, CA, USA*

**To whom correspondence should be addressed.*
M.N. Chan - Tel: (852) 3943-9863 E-mail: mnchan@cuhk.edu.hk
K.R. Wilson - Tel: (1) 510-495-2474 E-mail: krwilson@lbl.gov

Abstract

Oxygenated organic molecules are abundant in atmospheric aerosols and are transformed by oxidation reactions near the aerosol surface by gas-phase oxidants such as hydroxyl (OH) radicals. To gain better insights into how the structure of an organic molecule, particularly in the presence of hydroxyl groups, controls the heterogeneous reaction mechanisms of oxygenated organic compounds, this study investigates the OH-radical initiated oxidation of aqueous tartaric acid ($C_4H_6O_6$) droplets using an aerosol flow tube reactor. The molecular composition of the aerosols before and after reaction is characterized by a soft atmospheric pressure ionization source (Direct Analysis in Real Time, DART) coupled with a high resolution mass spectrometer. The aerosol mass spectra reveal that four major reaction products are formed: a single C_4 functionalization product ($C_4H_4O_6$) and three C_3 fragmentation products ($C_3H_4O_4$, $C_3H_2O_4$, and $C_3H_2O_5$). The C_4 functionalization product does not appear to originate from peroxy radical self-reactions, but instead forms via an α-hydroxylperoxy radical produced by a hydrogen atom abstraction by OH at the tertiary carbon site. The proximity of a hydroxyl group to peroxy group enhances the unimolecular HO_2 elimination from the α-hydroxylperoxy intermediate. This alcohol-to-ketone conversion yields 2-hydroxy-3-oxosuccinic acid ($C_4H_4O_6$), the major reaction product. While in general, C-C bond scission reacts are expected to dominate the chemistry of organic compounds with high average carbon oxidation states (OS_C), our results show that molecular structure can play a larger role the heterogeneous transformation of tartaric acid (OS_C = 1.5). These results are also compared with two structurally related dicarboxylic acids (succinic acid and 2,3-dimethylsuccinic acid) to elucidate how the identity and location of functional groups (methyl and hydroxyl groups) alters heterogeneous reaction mechanisms.

1. Introduction

Atmospheric aerosols are suspensions of small particles (solid or liquid) in air. These particles interact directly and indirectly with sunlight, affecting the Earth's radiation balance. Directly, aerosols absorb and scatter sunlight and affect the global radiative balance. Indirectly, they modify the size and number distribution of cloud droplets, altering how cloud droplets reflect and absorb sunlight.[1] Moreover, atmospheric aerosols can have adverse effects on our respiratory and cardiovascular systems.[2]

Atmospheric aerosols are chemically complex; composed of inorganic salts and a large variety of organic compounds. Organic compounds are a significant fraction (about 50%) of the mass of atmospheric aerosols[3] and can be oxidized at the aerosol surface by gas-phase hydroxyl radicals (OH), ozone (O_3), and nitrate radicals.[4] These heterogeneous oxidative processes continuously alter the surface and bulk composition of the aerosol, and thus modify aerosol properties such as light extinction, hygroscopicity and cloud condensation nuclei activity. [5-8]

The structure of an organic molecule (e.g. branching of the carbon backbone and average carbon oxidation state (OS_C)) plays a key role in controlling heterogeneous chemistry.[7, 9] Recently, we have investigated the heterogeneous OH oxidation of succinic acid and its more branched analog (2,3-dimethylsuccinic acid (2,3-DMSA)) to examine how branched methyl groups alter reaction mechanisms.[10, 11] Figure 1 shows reaction products with new oxygenated groups (i.e. "functionalization") are formed in the OH oxidation with succinic acid. The formation of these products are explained by the self-reactions of two peroxy radicals to form stable products (e.g. ketones and alcohols) via the Russell[12] and/or Bennett-Summer reaction mechanisms.[13] When the hydrogen atoms on succinic acid are substituted with methyl groups, as in the OH reaction with 2,3-DMSA (Figure 1), the two methyl groups sterically hinder the appropriate arrangement of two peroxy radicals into a cyclic tetroxide intermediate, which is necessary for the formation of stable ketone and alcohol products. Instead, alkoxy radicals are formed from peroxy radical self-reactions, and subsequently abstract hydrogen atoms from neighboring molecules to form alcohol functionalization products. Moreover, the abundance of these functionalization products is larger than the C-C bond scission fragmentation products. An opposite result is observed for succinic acid. These results illustrate how the differences in molecular structure can alter reaction pathways.

Recent studies suggest that fragmentation becomes more favorable when the degree of oxygenation (e.g. OS_C) of an organic molecule increases.[9, 14] However, a robust relationship between the degree of oxygenation and volatilization (a proxy for the fragmentation process) has not been established. For example, little aerosol carbon mass loss has been reported for more oxygenated citric acid (OS_C = 1), while a significant production of volatile products has been observed for less oxygenated erythritol (OS_C = -0.5) during OH oxidation.[15] Depending on the number, types and positions of the functional groups, organic compounds with the same or a similar degree of oxygenation (e.g. OS_C) can chemically evolve via distinct mechanisms.

To better understand how the molecular structure governs the heterogeneous chemistry of oxygenated organic aerosols, we investigate the OH initiated oxidation of tartaric acid ($C_4H_6O_6$) aerosols using an aerosol flow tube reactor. The composition of the aerosols before and after oxidation is characterized by a soft atmospheric pressure ionization source (Direct Analysis in Real Time, DART) coupled with a high resolution mass spectrometer in real time. Based on the identification of reaction products from exact mass measurements, we measure the oxidation kinetics and investigate reaction mechanisms, to examine how the presence of hydroxyl groups controls the competition between the functionalization and fragmentation pathways. Results from this work are compared with our previous studies (succinic acid and 2,3-DMSA) to examine more broadly how the identity of functional groups (methyl and hydroxyl groups) alter heterogeneous OH reaction mechanisms in these three structurally related dicarboxylic acids (Figure 1).

2. Method

2.1 Aerosol flow tube reactor

The heterogeneous OH oxidation of tartaric acid aerosols is investigated using an aerosol flow tube reactor. Experimental details have been described elsewhere.[10] In brief, aqueous droplets are first generated using a constant output atomizer (TSI Inc. Model 3076). The aerosol stream is then mixed with humidified nitrogen (N_2), oxygen (O_2), trace hexane, and O_3, and introduced to the reactor. The relative humidity (RH) measured at the inlet of the reactor is about 85.8 ± 0.26%. The temperature inside the reactor is maintained at 20°C using a circulating water jacket surrounding the reactor. Since neither deliquescence nor crystallization is observed for tartaric acid

aerosols,[16] we assume that the tartaric acid aerosols exist as aqueous droplets before oxidation. The size distribution of the droplets leaving the reactor is determined by a scanning mobility particle sizer (SMPS, TSI, 3936). Before oxidation, the mean surface weighted diameter for the droplets is measured to be 188.4 ± 0.5 nm. The initial aerosol mass loading is ~2800 μg m^{-3}. At RH = 85.8%, tartaric acid droplets are predicted to have a molarity of 3.27M and a mass fraction of solute (m_f) of 0.49.[17] The average density of the droplets (ρ) is estimated to be 1.38 g cm^{-3} using an additivity rule with the known density and mass fraction of tartaric acid and water.

Tartaric acid aerosols are oxidized by gas-phase OH radicals, which are generated by the photolysis of O_3 using ultraviolet lamps at 254 nm. The OH concentration is adjusted by varying the amount of O_3 added to the reactor and is quantified by measuring the consumption of a gas phase tracer (i.e. hexane) using a gas chromatography equipped with a flame ionization detector.[18] With a total flow rate of 2 L/min (an aerosol residence time of 1.3 min), the OH exposure (OH concentration × aerosol residence time) ranges from 0 to 4.63×10^{11} molecule cm^{-3} s (The method of measuring the OH exposure is described in Supporting Information). After exiting the reactor, the aerosol stream passes through an annular Carulite catalyst denuder to remove O_3 and an activated charcoal denuder to remove any gas-phase products. A portion of the aerosol stream is sampled by a SMPS for aerosol size measurements. The remaining flow is introduced into an ionization region, which is a narrow open space between a DART ionization source and an atmospheric inlet of a high resolution mass spectrometer (ThermoFisher, Q Exactive Orbitrap), for real time chemical characterization of the aerosols.

2.2 Atmospheric Pressure Aerosol Mass Spectrometer

The DART ionization source (IonSense: DART SVP)[19, 20] is operated in negative ionization mode with metastable helium as the ionizing reagent. The heater inside the DART ionization source is operated at 500ºC. Prior to entering the ionization region, the aerosols are vaporized in a heater to generate gas-phase species, which are then ionized by the DART source. Proton abstraction from the carboxyl group of tartaric acid and its reaction products produces the deprotonated molecular ions, $[M-H]^-$ observed in the aerosol mass spectra[21, 22] Detailed ionization mechanism is given in the Supporting Information. The resulting ions are sampled by the high resolution mass spectrometer. Mass spectra are collected at 1 s intervals over a scan range from

m/z 70 – 700. Each mass spectrum is averaged for 5 min. at a mass resolution of about 140,000. Mass calibration is performed with standard solutions before experiments. The mass spectra are analyzed using the Xcalibar software (Xcalibar Software, Inc., Herndon, VA, USA).

3. Results and Discussions

In the following sections, we first analyze the heterogeneous oxidative kinetics of tartaric acid (Section 3.1). Based on the aerosol mass spectra, reaction pathways are proposed (Section 3.2) to explain the formation of major reaction products and to explore the role of hydroxyl groups in the reaction mechanism. Finally, we discuss how different types of functional groups control the heterogeneous OH chemistry of three small structurally related dicarboxylic acids (succinic acid, 2,3-DMSA, and tartaric acid) (Section 3.3).

3.1 Oxidation Kinetics

Figure 2 shows that the reaction of OH with tartaric acid produces four major new peaks in the spectrum. The largest product peak corresponds to $C_4H_4O_6$; a C_4 functionalization product. The remaining peaks correspond to three distinct C_3 fragmentation products ($C_3H_4O_4$, $C_3H_2O_4$, and $C_3H_2O_5$). Figure 3A shows the reactive decay of tartaric acid (I/I_o) at different OH exposures. At the highest OH exposure (4.63×10^{11} molecule cm^{-3} s), about 60% of parent tartaric acid is consumed. The decay of tartaric acid is fit to an exponential function to obtain a second order heterogeneous OH reaction rate constant (k_{OH}).[18] k_{OH} is determined to be $(2.04\pm0.16) \times 10^{-12}$ cm^3 $molecule^{-1}$ s^{-1}. Using the fitted k_{OH} value, the effective OH uptake coefficient, γ_{OH}, defined as the fraction of OH collisions that yields a reaction, is computed using the following equation: [23]

$$\gamma_{OH} = \frac{2\, D_0\, \rho\, m_f\, N_A}{3\, M_w\, \overline{c_{OH}}}\, k_{OH} \qquad \text{(Eqn. 1)}$$

where D_0, and ρ are the mean surface weighted diameter and the density of the droplets before oxidation, respectively. M_w is the molecular weight of tartaric acid, m_f is mass fraction of solute in the droplets, N_A is Avogadro' number, and $\overline{c_{OH}}$ is the mean speed of gas-phase OH radicals. Using Eqn. 1, γ_{OH} is computed to be 1.16±0.19, which is larger than the value (0.40±0.13) reported by Kessler et al.[15] One possible explanation for this discrepancy is that the marker ion ($C_4H_2O_3^+$, *m/z* = 98) used by Kessler et al.[15] is not unique for tartaric acid but rather has contributions from

reaction products that fragment during the electron impaction ionization. This may lead to an overestimate of the concentration of unreacted tartaric acid, leading to smaller k_{OH}. However, a more likely explanation for this difference is the experimental conditions. Here the reaction is measured at a higher relative humidity (RH = 85.8%) than those of Kessler et al.[15] (RH = 30%). As shown by Davies and Wilson,[23] Houle et al.,[24] Slade and Knopf,[25] and Shiraiwa and coworkers, [26,27] the OH reactive uptake exhibits a complex dependence on aerosol viscosity, which in turn is controlled by RH. At high RH, tartaric acid aerosols are likely aqueous droplets with molecular components that can diffuse more rapidly to the aerosol surface for reaction with OH, leading to higher overall reaction rates.[10, 25] At low RH, the aerosols become more concentrated and viscous.[28] In this case, diffusion of the species from the bulk to the surface is slower and, thus tartaric acid in the interior of the aerosol is less likely to undergo oxidation at the surface. For example, Davies and Wilson[23] investigated the relationship between RH and the reactive uptake of OH radicals onto citric acid ($C_6H_8O_7$) droplets. They observed that the γ_{OH} decreases by about a factor of 2 (~0.112 to ~0.052) when the RH decreases from 90% to 20%, and suggested that at low humidity the reactive OH decay of citric acid is controlled by aerosol viscosity, with reactions occurring near the aerosol/air interface. More work is needed to elucidate the effect of humidity on the heterogeneous oxidative kinetics of tartaric acid.

3.2 Reaction Mechanisms

Based on the aerosol mass spectra and previously reported aerosol-phase reaction pathways,[5, 29] reaction schemes are proposed to explain the formation of the major products observed in Figure 2. Figure 3B shows the kinetic evolution of these reaction products at different OH exposures. The relative abundance of all products increases with OH exposure and reaches a maximum at the highest OH exposure. To the best of our knowledge, authentic standards or surrogates are not available for these reaction products. As a first approximation, the ionization efficiencies of tartaric acid and all products are assumed to be equal. We acknowledge that certain products (e.g., organic peroxides and oligomers) may not be detected efficiently by the DART.[10, 11]

3.2.1 OH oxidation of tartaric acid: first generation products

Scheme 1A shows the OH oxidation with tartaric acid can be initiated by hydrogen abstraction at either a tertiary backbone carbon site (Scheme 1A: *Path IA*) or a hydroxyl group (Scheme 1A: *Path IB*). When the hydrogen abstraction occurs on the tertiary carbon site (Scheme 1A: *Path IA*), an alkyl radical forms and reacts quickly with O_2 to form an α-hydroxylperoxy radical, which can undergo unimolecular HO_2 elimination to form 2-hydroxy-3-oxosuccinic acid ($C_4H_4O_6$), the major functionalization product observed in the aerosol mass spectrum. The relative abundance of this product is 16.5% at an OH exposure = 4.63 x 10^{11} molecule cm^{-3} s (Figure 3B). As illustrated in Scheme 2A, an α-hydroxylperoxy radical can adopt a cyclic transition state and yield a carbonyl product together with a HO_2 radical, which can further dissociate into H^+ and $O_2^{\cdot-}$ in an aqueous solution.[30] Bothe et al.[30-32] examined the OH reaction with a series of alcohols with differing numbers of hydroxyl groups in dilute aqueous solution. They found that alcohols with multiple hydroxyl groups (e.g. meso-erythritol, methyl α-D-glucoside, and D-xylitol) exhibit faster unimolecular HO_2 elimination rates (k_{HO_2}= 2000 - 3000 s^{-1}) than alcohols with a single hydroxyl group (e.g. methanol, ethanol, and propan-2-ol) (k_{HO_2} = <10 - 650 s^{-1}). They proposed that for polyols, the hydroxyl group adjacent to the peroxy group can stabilize the resultant carbonyl group by forming strong intramolecular hydrogen bond, thus enhancing the unimolecular HO_2 elimination rate. As shown in Scheme 2B, the unimolecular HO_2 elimination from the α-hydroxylperoxy radical formed on tartaric acid may be similarly enhanced due to hydrogen bonding to the hydroxyl group located at the β-position of the peroxy group.

In addition to unimolecular HO_2 elimination, the α-hydroxylperoxy radical can in principle react with another peroxy radical. However, reaction products (see Scheme 1) formed from these self-reactions are not detected. For example, the self-reactions of two peroxy radicals can yield two alkoxy radicals, which can decompose to form tartronic acid ($C_3H_4O_5$) and oxalic acid ($C_2H_2O_4$). Similar to tartaric acid, these two dicarboxylic acids should be easily ionized by DART if produced in significant quantities. For example, we previously detected the formation of oxalic acid in the OH oxidation of succinic acid.[10] Furthermore, the effective vapor pressure (c^*) of tartronic acid and oxalic acid is estimated to be about 12 and 797 μg m^{-3}, respectively, using the saturation vapor pressures reported in the literature.[33, 34] As a first approximation, assuming an equilibrium gas/aerosol partitioning, a significant mass fraction of tartronic acid (99.6%) and oxalic acid (78.2%) would remain in the aerosol-phase under our experimental conditions. The

absence of these two products in the aerosol mass spectra further supports that rapid unimolecular HO_2 elimination is the dominant reactor pathway for the α-hydroxylperoxy radical. [35]

When hydrogen abstraction occurs on the hydroxyl group (Scheme 1A: *Path IB*), the resultant alkoxy radical can decompose to form 2-hydroxy-3-oxopropanoic acid ($C_3H_4O_4$), which is one of the major fragmentation products seen in Figure 2 and contributes to about 6.6% of the total ion signal at OH exposure = 4.63 x 10^{11} molecule cm^{-3} s (Figure 3B). Although the bond energy of O-H is typically larger than that of C-H,[36] the detection of 2-hydroxy-3-oxopropanoic acid suggests that the hydrogen abstraction on the hydroxyl group likely occurs. In competition with decomposition, the alkoxy radical can react with O_2 to form the functionalization product, 2-hydroxy-3-oxosuccinic acid ($C_4H_4O_6$), or abstract a hydrogen atom from a neighbouring molecule.

As a first approximation, the concentration of dissolved O_2 ($[O_2]_{aq}$) is in the order of 10^{17} molecule cm^{-3} under one atmospheric pressure based on the Henry's law constant. Taking a second-order O_2 reaction with an alkoxy radical as 10^{-14} cm^3 $molecule^{-1}$ s^{-1}, suggested by Atkinson et al.,[37] the pseudo first-order rate constant ($k_{O_2}[O_2]_{aq}$) is estimated to be about 10^3 s^{-1}. For the intermolecular hydrogen abstraction, the concentration of the molecules available for hydrogen abstraction, [RH], is assumed to be equal to that of tartaric acid before oxidation ([RH] is in order of 10^{21} molecule cm^{-3}). The hydrogen abstraction rate of an alkoxy radical is estimated to be 10^{-16} cm^3 $molecule^{-1}$ s^{-1}.[38] This gives the pseudo first-order rate constant (k_{RO+RH} [RH]) of about 10^5 s^{-1}. The unimolecular decomposition rate of an alkoxy radical, k_{des}, can be estimated using a structural activity relationships (SAR) proposed for the decomposition of gas-phase alkoxy radicals.[39, 40] The SAR model predicts a large k_{des} (10^{13} s^{-1}) because the hydroxyl and carbonyl groups on the leaving radicals greatly enhance radical stability and lower the energy barrier for decomposition. This simple analysis suggests that when the hydrogen abstraction occurs on the hydroxyl group, the resultant alkoxy radical will most likely decompose to form 2-hydroxy-3-oxopropanoic acid ($C_3H_4O_4$, Scheme 1A: *Path IB*), while hydrogen abstraction at the tertiary carbon site forms 2-hydroxy-3-oxosuccinic acid ($C_4H_4O_6$) produced via unimolecular HO_2 elimination from the α-hydroxylperoxy intermediate (Scheme 1A: *Path IA*).

It is also potentially possible that hydrogen abstraction might occur on the OH group of the carboxylic acid. This process could lead to the decarboxylation of the acid and after subsequent

addition of O_2 to the resulting radical form a primary α-hydroxylperoxy intermediate, which can in turn eliminate HO_2 to produce 2-hydroxy-3-oxopropanoic acid ($C_3H_4O_4$). However, abstracting a hydrogen atom from the carboxyl group is expected to be less favorable than from the hydroxyl group.[41]

3.2.2 OH Oxidation of 2-hydroxy-3-oxosuccinic acid: Second-generation products

When the reaction proceeds further, 2-hydroxy-3-oxosuccinic acid ($C_4H_4O_6$), the most abundant first generation product, can be oxidized to form two minor fragmentation products ($C_3H_2O_4$ and $C_3H_2O_5$). As shown in Scheme 1B, for the OH reaction with 2-hydroxy-3-oxosuccinic acid, there are two hydrogen atoms available for abstraction: one at the tertiary carbon site (Scheme 1B: *Path IIA*) and one from the hydroxyl group (Scheme 1B: *Path IIB*). When the abstraction occurs on the tertiary carbon site (Scheme 1B*: Path IIA*), an O_2 molecule can quickly react with an alkyl radical to form an α-hydroxylperoxy radical. However, in contrast to the α-hydroxylperoxy radical formed from the OH oxidation with tartaric acid (Scheme 1A: *Path IA*), the product of unimolecular HO_2 elimination, dioxosuccinic acid ($C_4H_2O_6$), is not observed (Scheme 1B: *Path IIA*). Instead, an ion in the aerosol mass spectrum corresponding to mesoxalic acid ($C_3H_2O_5$) is detected (Figure 2). The most likely formation route for mesoxalic acid ($C_3H_2O_5$) is the reaction of the α-hydroxylperoxy radical with another peroxy radical to form two tertiary alkoxy radicals, which in turn decompose to form mesoxalic acid ($C_3H_2O_5$).

This difference between first and second generation products originating from the same type of α-hydroxylperoxy intermediate can be explained by differences in molecular structure. The carbonyl, on the second generation α-hydroxylperoxy radical (Scheme 1B: *Path IIA*), adjacent to the peroxy group, cannot form an intramolecular hydrogen bond with resulting carbonyl group in the reaction product (shown in Scheme 2C). Thus, it is likely that the peroxy radical formed on 2-hydroxy-3-oxosuccinic acid exhibits much slower unimolecular HO_2 elimination rates than that of tartaric acid. For OH reactions with alcohols with single or multiple hydroxyl groups, Bothe et al.[30-32] reported that the unimolecular HO_2 elimination rates are slowed by one to three orders of magnitude in an absence of a hydroxyl group adjacent to the peroxy group. These results illustrate how molecular structure (i.e. the potential for intramolecular hydrogen bond formation) plays a

key role in governing the competition between unimolecular (HO_2 elimination) and bimolecular ($RO_2 + RO_2$) reaction steps in aqueous tartaric acid aerosol reactions.

When the hydrogen atom on the hydroxyl group is removed by the OH radical (Scheme 1B: *Path IIB*), an activated tertiary alkoxy radical forms. The decomposition product of this alkoxy radical is 2,3-dioxopropanoic acid ($C_3H_2O_4$). This is expected, since the decomposition rate of the activated alkoxy radicals is estimated to be very fast ($\sim 10^{11}$ s^{-1}).[39, 40] Like tartaric acid, the intermolecular hydrogen abstraction ($\sim 10^5$ s^{-1}) and O_2 reaction with the alkoxy radical ($\sim 10^3$ s^{-1}) are predicted to be much less competitive with the decomposition of the alkoxy radical for 2-hydroxy-3-oxosuccinic acid.

The kinetic measurements show that γ_{OH} (1.16±0.19) is slightly larger than one, suggesting the possibility of secondary chemistry. One possibility for radical chain propagation is the intermolecular hydrogen abstraction by an alkoxy radical (RO+RH). However, the time constant analysis presented above suggests that this reaction rate does not compete with decomposition since in each case activated alkoxy radicals are formed. This is in contrast to the formation of alkoxy radical in chemical reduced systems (e.g. alkanes) which preferentially react via intermolecular hydrogen abstraction (i.e. RO + RH).[42] Another possibility for radical chain propagation chemistry that is consistent with the mechanism outlined above is the formation and subsequent reaction of $O_2^{\cdot-}$ ions. These species are formed from the dissociation of HO_2 radicals and may abstract hydrogen atoms from tartaric acid and its reaction products.[43] However, it is noted that the *in situ* acidity of tartaric acid droplets is not known. At 85% RH, the concentration of tartaric acid is about 3.27M. From the acidity constants (pK_{a1} = 2.89 and pK_{a2} = 4.40), the pH of the droplets is calculated to be 1.03. While HO_2 radicals (pK_a = 4.8) can dissociate into H^+ and $O_2^{\cdot-}$ in a dilute aqueous solution under highly acidic environment, it is unclear that HO_2 will fully dissociate in the concentrated tartaric acid droplets. Since hydrogen abstraction rates are not well constrained for tartaric acid and its observed products, more work is needed to investigate the role of $O_2^{\cdot-}$ reactions in the OH oxidation of aqueous tartaric acid droplets. This reaction pathway is not considered in reaction schemes.

3.2.3. OH reaction site: Tertiary backbone carbon site vs. hydroxyl group

As discussed in the preceding sections (3.2.1 and 3.2.2), hydrogen atoms on the tertiary backbone carbon site and the hydroxyl group can be abstracted by OH radicals. As shown in Table 1 and Scheme 1, depending on the OH reaction site, reaction products with distinct chemical formula are formed and can be assembled into two separate groups (tertiary carbon site vs. hydroxyl group). The ratio of the abundance of reaction products in these two groups corresponds to the ratio of OH attacks at the tertiary carbon site and the hydroxyl group. When the hydrogen abstraction occurs at the tertiary carbon site of tartaric acid, 2-hydroxy-3-oxosuccinic acid ($C_4H_4O_6$) is formed as the major functionalization product (Scheme 1A: *Path IA*). Since 2-hydroxy-3-oxosuccinic acid ($C_4H_4O_6$) can be further oxidized to yield two fragmentation products (2,3-dioxopropanoic acid ($C_3H_2O_4$) and mesoxalic acid ($C_3H_2O_5$)) (Scheme 1B), these two second-generation products originate from the OH reaction at the tertiary carbon site of tartaric acid. 2-hydroxy-3-oxopropanoic acid ($C_3H_4O_4$) is the only product that can be attributed to hydrogen abstraction at the hydroxyl group (Scheme 1A: *Path IB*) in tartaric acid. As shown in Figure 3B, the total abundance of reaction products originating from the tertiary carbon site is larger than that originated from the hydroxyl group. For example, at the maximum OH exposure, the tertiary carbon site vs. hydroxyl group products ratio is about 3.3. The results of this simple analysis suggest that the tertiary carbon site is the preferential OH reaction site and are consistent with differences in relative strengths of C-H bond (tertiary carbon site) and O-H bond (hydroxyl group)[36].

3.2.4 Volatilization of oxidized tartaric acid aerosols

Using the detailed molecular information obtained for the reaction products, further insight into how oxidation alters the properties of the aerosol (e.g. volatility) can be investigated. Kessler et al.[15] measured the volatilization of tartaric acid aerosols during the heterogeneous OH oxidation. At the OH exposure of ~10^{11} molecule cm^{-3} s, which is close to the maximum OH exposure investigated in our study, a small quantity of aerosol carbon mass loss (< 2%) was observed. About 10% of total aerosol carbon mass is lost at the highest OH exposure in their measurements (~10^{12} molecule cm^{-3} s). They suggested that fragmentation products may have sufficiently low volatilities to remain in the aerosol-phase. Based on proposed reaction schemes and the molecular structures of the reaction products, the saturation vapor pressures of the products are predicted

using the group contribution method developed by Pankow and Asher.[44] The c^* of the fragmentation products are predicted to be in the order of 10^2 to 10^4 μg m^{-3} (Table 1). These results support Kessler et al.'s observation that a significant fraction of fragmentation products remain in the aerosol-phase given the organic aerosol loading is about 500-650 μg m^{-3} in their measurements. Equilibrium gas/aerosol partitioning calculations predict here that about 36-42% of 2-hydroxy-3-oxopropanoic acid ($C_3H_4O_4$) and 81-85% of mesoxalic acid ($C_3H_2O_5$) remain in the aerosol-phase, while 2,3-dioxopropanoic acid ($C_3H_2O_4$) is a volatile product (only < 5% remains in aerosol-phase). It is noted that the reaction products might expect to be less volatile than predicted. For example, the saturation vapor pressure of tartaric acid is reported to be $(1.8\text{-}4.9)\times10^{-8}$ Pa,[45] while the modeled value is 2×10^{-7} Pa.[44] Moreover, as shown in Figure 3C, if we assume the ionization efficiencies of all observed products are the same and the major reaction products can be ionized by the DART ionization source, the abundance of functionalization product is found to be slightly larger than that of fragmentation products. Our results further suggest that a small aerosol carbon mass loss reported in the literature could also attribute to the formation of nonvolatile functionalization product (c^* of 2-hydroxy-3-oxosuccinic acid is predicted to be 0.315 μg m^{-3}).

3.3 Effect of Different Functional Groups on the Heterogeneous Reaction Mechanisms

The structure of an organic molecule plays a key role in controlling the heterogeneous chemistry. The evolution in molecular composition of the reaction products formed in the heterogeneous OH reaction with succinic acid,[10] 2,3-DMSA,[11] and tartaric acid is used to examine how different functional groups determines the heterogeneous reaction mechanisms for these three structurally related dicarboxylic acids (Figure 1).[46]

The change in average aerosol elemental composition upon oxidation can be expressed in term of hydrogen-to-carbon ratio (H/C), oxygen-to-carbon ratio (O/C), carbon oxidation state ($OS_C = 2\times(O/C) - (H/C)$)[47] and average carbon number (N_C). These quantities are computed from the relative abundance and suggested chemical formula of the observed products:

$$Q_{avg} = \sum_i Q_i I_i \qquad \text{(Eqn. 3)}$$

where Q can be H/C, O/C, OS_C or N_C. Q_{avg} is the average quantity. Q_i and I_i are the quantity and relative abundance of the reaction product i, respectively. As shown in Figure 4A, when the OH exposure increases, the OS_C increases and the N_C decreases for all three acids. However, the acids exhibit different oxidation pathways in the van Krevelen plot (H/C vs. O/C) (Figure 4B). At a similar OH exposure (about 4×10^{11} cm^3 $molecule^{-1}s^{-1}$), a slope of about -1 is observed for succinic acid (-0.88) and 2,3-DMSA (-0.72), but a steep positive slope of +13.6 is observed for tartaric acid. Aerosol speciation data further reveal that the acids have different molecular distribution of reaction products. For succinic acid (Figures 5C and 5D), the bulk aerosol elemental composition evolves largely through the formation of smaller fragmentation products with higher oxidation states. In contrast to succinic acid, for both tartaric acid (Figures 5A and 5B) and 2,3-DMSA (Figures 5E and 5F), only a few major products are formed. Both functionalization products and fragmentation products contribute significantly to the observed products. All these results suggest that the acids chemically evolve via distinct mechanisms.

For the OH reaction with succinic acid (Figure 1B), we found that the ketone-to-alcohol (i.e. functionalization products) ratio is about 1 and can be explained by self-reactions of two peroxy radicals via the Bennett-Summers reaction[13] or Russell mechanism.[12] These two mechanisms have also been suggested to be major formation pathways of functionalization products in the OH oxidation of C_2 - C_9 unsubstituted dicarboxylic acids.[35,46,48] On the other hand, when the methyl or hydroxyl groups are substituted to the backbone of succinic acid, the functionalization products are formed via different pathways and the relative importance of functionalization vs. fragmentation processes increases. With the presence of two methyl groups in 2,3-DMSA (Figure 1C), the ketone-to-alcohol functionalization products ratio drops to near 0 (i.e. no ketone functionalization product is formed). It is hypothesized that the two bulky methyl groups may sterically hinder the appropriate arrangement of two peroxy radicals into the correct intermediate, necessary for the formation of functionalization products proposed in the Russell mechanism. Alternatively, alkoxy radicals are produced from these self-reactions and can in turn abstract hydrogen atoms from neighboring molecules to form the alcohol functionalization products. It is also postulated that the methyl groups might enhance the stability of the tertiary alkoxy radicals. This may favor the intermolecular hydrogen abstraction and in part explain the

significant formation of functionalization products (Figures 5E and 5F).[11] However, more work is needed to test this hypothesis.

For tartaric acid (Figure 1A), the formation of functionalization products does not appear to proceed through bimolecular reactions of two peroxy radicals. In presence of a hydroxyl group near the peroxy group, the α-hydroxylperoxy radical tends to undergo the unimolecular HO_2 elimination process (Scheme 2B). This functionalization process converts an alcohol group to a ketone group (the ketone-to-alcohol functionalization products ratio tends to infinity), leading to a high abundance of functionalization products (Figures 5A and 5B). Since the functionalization product contribute significantly to the observed products, the steep, positive slope observed in the van Krevelen plot arise from the conversion of alcohols to ketones originating from unimolecular HO_2 elimination during oxidation.[35]

Overall, for these three structurally related acids, the fragmentation products appear to be primarily formed through the decomposition of alkoxy radicals while the functionalization products are formed via distinct pathways. At the same OH exposure, the relative contribution of fragmentation products to the total products is less significant for 2,3-DMSA and tartaric acid when compared to succinic acid. This observation does not agree with recent hypothesis that the fragmentation process is more important for more branched and oxygenated species relative to their less branched and oxygenated analogs.[49] These results show that the types and location of the functional groups (e.g. methyl and hydroxyl groups) can significantly alter reaction pathways for these two structurally related dicarboxylic acids.

4. Conclusions

In this work, we investigate the chemical evolution in the composition of aqueous tartaric acid droplets during the heterogeneous OH oxidation. The aerosol speciation data have revealed that the functionalization products are the most abundant among the observed products. This can be explained by that when the tertiary backbone carbon site of tartaric acid is abstracted by the OH radical, the presence of a hydroxyl group on the neighboring position of the peroxy group favors the unimolecular HO_2 elimination of the α-hydroxylperoxy radical over the self-reactions of two peroxy radicals. This functionalization process converts an alcohol group into a ketone group,

yielding 2-hydroxy-3-oxosuccinic acid. On the other hand, when the hydrogen atom from the backbone carbon site of 2-hydroxy-3-oxosuccinic acid is abstracted by the OH radical, in the absence of a hydroxyl group adjacent to the peroxy group, the bimolecular reaction of two peroxy radicals becomes competitive with the unimolecular HO_2 elimination process. The alkoxy radical resulted from peroxy radical self-reactions tend to decompose, leading to a fragmentation of the carbon backbone. Although higher bond dissociation energy is expected for the O-H bond than the C-H bond, a significant fraction of fragmentation products are likely produced through the decomposition of alkoxy radicals resulted from the hydrogen abstraction on the hydroxyl group.

Both functionalization and fragmentation products contribute significantly to the observed products in the OH oxidation of tartaric acid. This is not consistent with recent hypothesis that the fragmentation process is expected to be favorable for oxygenated organic compounds. The results of this work may suggest that for oxygenated organic compounds, especially those with multiple hydroxyl groups, the position of the hydroxyl groups may play a role in determining the competitions between functionalization and fragmentation processes during oxidation. In addition to the bulk elemental composition such as O/C and OS_C, results from this work and our previous studies suggest that the number, types and location of the functional groups (e.g. hydroxyl, ketone, and carboxyl groups) is needed to better understand the heterogeneous chemistry.

5. Supporting Information

The Supporting Information is available free of charge on the ACS Publications website at DOI: Experimental details, including the measurement of OH exposure and ionization mechanism of DART source.

6. Acknowledgement

C.T. Cheng and M.N. Chan are supported by a Direct Grant for Research (4053089) and One-Time Funding Allocation of Direct Grant (3132765), The Chinese University of Hong Kong. K.R. Wilson and the experimental research facilities are supported by the Department of Energy, Office of Science Early Career Award and the Director, Office of Energy Research, Office of Basic

Energy Sciences, Chemical Sciences, Geosciences, and Biosciences Division of the U.S. Department of Energy under Contract No. DE-AC02-05CH11231.

7. References

1. Hallquist, M.; Wenger, J. C.; Baltensperger, U.; Rudich, Y.; Simpson, D.; Claeys, M.; Dommen, J.; Donahue, N. M.; George, C.; Goldstein, A. H., et al. The Formation, Properties and Impact of Secondary Organic Aerosol: Current and Emerging Issues. *Atmos. Chem. Phys.* **2009,** *9*, 5155-5236.
2. Pope III, C. A.; Dockery, D. W. Health Effects of Fine Particulate Air Pollution: Lines That Connect. *J. Air Waste Manage.* **2006,** *56*, 709-742.
3. Ng, N. L.; Canagaratna, M. R.; Jimenez, J. L.; Chhabra, P. S.; Seinfeld, J. H.; Worsnop, D. R. Changes in Organic Aerosol Composition with Aging Inferred from Aerosol Mass Spectra. *Atmos. Chem. Phys.* **2011,** *11*, 6465-6474.
4. Rudich, Y.; Donahue, N. M.; Mentel, T. F. Aging of Organic Aerosol: Bridging the Gap between Laboratory and Field Studies. *Annu. Rev. Phys. Chem.* **2007,** *58*, 321-352.
5. George, I. J.; Abbatt, J. P. Heterogeneous Oxidation of Atmospheric Aerosol Particles by Gas-Phase Radicals. *Nat. Chem.* **2010,** *2*, 713-722.
6. Cappa, C. D.; Che, D. L.; Kessler, S. H.; Kroll, J. H.; Wilson, K. R. Variations in Organic Aerosol Optical and Hygroscopic Properties Upon Heterogeneous OH Oxidation. *J. Geophys. Res. Atmos.* **2011,** *116*.
7. Jimenez, J. L.; Canagaratna, M. R.; Donahue, N. M.; Prevot, A. S.; Zhang, Q.; Kroll, J. H.; DeCarlo, P. F.; Allan, J. D.; Coe, H.; Ng, N. L., et al. Evolution of Organic Aerosols in the Atmosphere. *Science* **2009,** *326*, 1525-1529.
8. Petters, M. D.; Prenni, A. J.; Kreidenweis, S. M.; DeMott, P. J.; Matsunaga, A.; Lim, Y. B.; Ziemann, P. J. Chemical Aging and the Hydrophobic-to-Hydrophilic Conversion of Carbonaceous Aerosol. *Geophys. Res. Lett.* **2006,** *33*.
9. Kroll, J. H.; Smith, J. D.; Che, D. L.; Kessler, S. H.; Worsnop, D. R.; Wilson, K. R. Measurement of Fragmentation and Functionalization Pathways in the Heterogeneous Oxidation of Oxidized Organic Aerosol. *Phys. Chem. Chem. Phys.* **2009,** *11*, 8005-8014.
10. Chan, M. N.; Zhang, H. F.; Goldstein, A. H.; Wilson, K. R. Role of Water and Phase in the Heterogeneous Oxidation of Solid and Aqueous Succinic Acid Aerosol by Hydroxyl Radicals. *J. Phys. Chem. C* **2014,** *118*, 28978-28992.
11. Cheng, C. T.; Chan, M. N.; Wilson, K. R. The Role of Alkoxy Radicals in the Heterogeneous Reaction of Two Structural Isomers of Dimethylsuccinic Acid. *Phys. Chem. Chem. Phys.* **2015,** *17*, 25309-25321.
12. Russell, G. A. Deuterium-Isotope Effects in the Autoxidation of Aralkyl Hydrocarbons. Mechanism of the Interaction of Peroxy Radicals. *J. Am. Chem. Soc.* **1957,** *79*, 3871-3877.
13. Bennett, J. E.; Summers, R. Product Studies of the Mutual Termination Reactions of Sec-Alkylperoxy Radicals: Evidence for Non-Cyclic Termination. *Can. J. Chem.* **1974,** *52*, 1377-1379.
14. Chacon-Madrid, H. J.; Donahue, N. M. Fragmentation Vs. Functionalization: Chemical Aging and Organic Aerosol Formation. *Atmos. Chem. Phys.* **2011,** *11*, 10553-10563.

15. Kessler, S. H.; Nah, T.; Daumit, K. E.; Smith, J. D.; Leone, S. R.; Kolb, C. E.; Worsnop, D. R.; Wilson, K. R.; Kroll, J. H. OH-Initiated Heterogeneous Aging of Highly Oxidized Organic Aerosol. *J. Phys. Chem. A* **2012,** *116*, 6358-6365.
16. Peng, C.; Chan, M. N.; Chan, C. K. The Hygroscopic Properties of Dicarboxylic and Multifunctional Acids: Measurements and UNIFAC Predictions. *Environ. Sci. Technol.* **2001,** *35*, 4495-4501.
17. Zuend, A.; Marcolli, C.; Luo, B. P.; Peter, T. A Thermodynamic Model of Mixed Organic-Inorganic Aerosols to Predict Activity Coefficients. *Atmos. Chem. Phys.* **2008,** *8*, 4559-4593.
18. Smith, J. D.; Kroll, J. H.; Cappa, C. D.; Che, D. L.; Liu, C. L.; Ahmed, M.; Leone, S. R.; Worsnop, D. R.; Wilson, K. R. The Heterogeneous Reaction of Hydroxyl Radicals with Sub-Micron Squalane Particles: A Model System for Understanding the Oxidative Aging of Ambient Aerosols. *Atmos. Chem. Phys.* **2009,** *9*, 3209-3222.
19. Cody, R. B.; Laramee, J. A.; Durst, H. D. Versatile New Ion Source for the Analysis of Materials in Open Air under Ambient Conditions. *Anal. Chem.* **2005,** *77*, 2297-2302.
20. Cody, R. B. Observation of Molecular Ions and Analysis of Nonpolar Compounds with the Direct Analysis in Real Time Ion Source. *Anal. Chem.* **2008,** *81*, 1101-1107.
21. Chan, M. N.; Nah, T.; Wilson, K. R. Real Time in Situ Chemical Characterization of Sub-Micron Organic Aerosols Using Direct Analysis in Real Time Mass Spectrometry (DART-MS): The Effect of Aerosol Size and Volatility. *Analyst* **2013,** *138*, 3749-3757.
22. Nah, T.; Chan, M.; Leone, S. R.; Wilson, K. R. Real Time in Situ Chemical Characterization of Submicrometer Organic Particles Using Direct Analysis in Real Time-Mass Spectrometry. *Anal. Chem.* **2013,** *85*, 2087-2095.
23. Davies, J. F.; Wilson, K. R. Nanoscale Interfacial Gradients Formed by the Reactive Uptake of OH Radicals onto Viscous Aerosol Surfaces. *Chem. Sci.* **2015,** *6*, 7020-7027.
24. Houle, F. A.; Hinsberg, W. D.; Wilson, K. R. Oxidation of a Model Alkane Aerosol by OH Radical: The Emergent Nature of Reactive Uptake. *Phys. Chem. Chem. Phys.* **2015,** *17*, 4412-4423.
25. Slade, J. H.; Knopf, D. A. Multiphase OH Oxidation Kinetics of Organic Aerosol: The Role of Particle Phase State and Relative Humidity. *Geophys. Res. Lett.* **2014,** *41*, 5297-5306.
26. Berkemeier, T.; Huisman, A. J.; Ammann, M.; Shiraiwa, M.; Koop, T.; Pöschl, U. Kinetic Regimes and Limiting Cases of Gas Uptake and Heterogeneous Reactions in Atmospheric Aerosols and Clouds: A General Classification Scheme. *Atmos. Chem. Phys.* **2013,** *13*, 6663-6686.
27. Arangio, A. M.; Slade, J. H.; Berkemeier, T.; Pöschl, U.; Knopf, D. A.; Shiraiwa, M. Multiphase Chemical Kinetics of OH Radical Uptake by Molecular Organic Markers of Biomass Burning Aerosols: Humidity and Temperature Dependence, Surface Reaction, and Bulk Diffusion. *J. Phys. Chem. A* **2015,** *119*, 4533-4544.
28. Parmar, M. L.; Awasthi, R. K.; Guleria, M. K. A Study on Viscosities of Citric Acid and Tartaric Acid in Water and Binary Aqueous Mixtures of Ethanol at Different Temperatures. *Indian J. Chem. A* **2004,** *43*, 41-44.
29. Leitner, N. K. V.; Dore, M. Hydroxyl Radical Induced Decomposition of Aliphatic Acids in Oxygenated and Deoxygenated Aqueous Solutions. *J. Photoch. Photobio. A* **1996,** *99*, 137-143.
30. Bothe, E.; Behrens, G.; Schulte-Frohlinde, D. Mechanism of the First Order Decay of 2-Hydroxy-Propyl-2-Peroxyl Radicals and of O2· Formation in Aqueous Solution. *Z. Naturforsch. B* **1977,** *32*, 886-889.

31. Bothe, E.; Schuchmann, M. N.; Schulte-Frohlinde, D.; von Sonntag, C. HO2 Elimination from A-Hydroxyalkylperoxyl Radicals in Aqueous Solution. *Photochem. Photobiol.* **1978,** *28*, 639-643.
32. Bothe, E.; Schulte-Frohlinde, D.; von Sonntag, C. Radiation Chemistry of Carbohydrates. Part 16. Kinetics of HO2 Elimination from Peroxyl Radicals Derived from Glucose and Polyhydric Alcohols. *J. Chem. Soc. Perk. T. 2* **1978**, 416-420.
33. Booth, A. M.; Montague, W. J.; Barley, M. H.; Topping, D. O.; McFiggans, G.; Garforth, A.; Percival, C. J. Solid State and Sub-Cooled Liquid Vapour Pressures of Cyclic Aliphatic Dicarboxylic Acids. *Atmos. Chem. Phys.* **2011,** *11*, 655-665.
34. Donahue, N.; Robinson, A.; Stanier, C.; Pandis, S. Coupled Partitioning, Dilution, and Chemical Aging of Semivolatile Organics. *Environ. Sci. Technol.* **2006,** *40*, 2635-2643.
35. Charbouillot, T.; Gorini, S.; Voyard, G.; Parazols, M.; Brigante, M.; Deguillaume, L.; Delort, A.-M.; Mailhot, G. Mechanism of Carboxylic Acid Photooxidation in Atmospheric Aqueous Phase: Formation, Fate and Reactivity. *Atmos. Environ.* **2012,** *56*, 1-8.
36. Blanksby, S. J.; Ellison, G. B. Bond Dissociation Energies of Organic Molecules. *Accounts Chem. Res.* **2003,** *36*, 255-263.
37. Atkinson, R. Rate Constants for the Atmospheric Reactions of Alkoxy Radicals: An Updated Estimation Method. *Atmos. Environ.* **2007,** *41*, 8468-8485.
38. Denisov, E. T.; Afanas' ev, I. B. *Oxidation and Antioxidants in Organic Chemistry and Biology*. CRC press: United States, 2005.
39. Peeters, J.; Fantechi, G.; Vereecken, L. A Generalized Structure-Activity Relationship for the Decomposition of (Substituted) Alkoxy Radicals. *J. Atmos. Chem.* **2004,** *48*, 59-80.
40. Vereecken, L.; Peeters, J. Decomposition of Substituted Alkoxy Radicals-Part I: A Generalized Structure-Activity Relationship for Reaction Barrier Heights. *Phys. Chem. Chem. Phys.* **2009,** *11*, 9062-9074.
41. Monod, A.; Doussin, J. F. Structure-Activity Relationship for the Estimation of OH-Oxidation Rate Constants of Aliphatic Organic Compounds in the Aqueous Phase: Alkanes, Alcohols, Organic Acids and Bases. *Atmos. Environ.* **2008,** *42*, 7611-7622.
42. Wiegel, A. A.; Wilson, K. R.; Hinsberg, W. D.; Houle, F. A. Stochastic Methods for Aerosol Chemistry: A Compact Molecular Description of Functionalization and Fragmentation in the Heterogeneous Oxidation of Squalane Aerosol by OH Radicals. *Phys. Chem. Chem. Phys.* **2015,** *17*, 4398-4411.
43. Hayyan, M.; Hashim, M. A.; AlNashef, I. M. Superoxide Ion: Generation and Chemical Implications. *Chem. Rev.* **2016**, 3029-3085.
44. Pankow, J. F.; Asher, W. E. SIMPOL.1: A Simple Group Contribution Method for Predicting Vapor Pressures and Enthalpies of Vaporization of Multifunctional Organic Compounds. *Atmos. Chem. Phys.* **2008,** *8*, 2773-2796.
45. Huisman, A. J.; Krieger, U. K.; Zuend, A.; Marcolli, C.; Peter, T. Vapor Pressures of Substituted Polycarboxylic Acids Are Much Lower Than Previously Reported. *Atmos. Chem. Phys.* **2013,** *13*, 6647-6662.
46. Yang, L.; Ray, M. B.; Yu, L. E. Photooxidation of Dicarboxylic Acids—Part II: Kinetics, Intermediates and Field Observations. *Atmos. Environ.* **2008,** *42*, 868-880.

47. Kroll, J. H.; Donahue, N. M.; Jimenez, J. L.; Kessler, S. H.; Canagaratna, M. R.; Wilson, K. R.; Altieri, K. E.; Mazzoleni, L. R.; Wozniak, A. S.; Bluhm, H., et al. Carbon Oxidation State as a Metric for Describing the Chemistry of Atmospheric Organic Aerosol. *Nat. Chem.* **2011,** *3*, 133-139.
48. Enami, S.; Hoffmann, M. R.; Colussi, A. J. Stepwise Oxidation of Aqueous Dicarboxylic Acids by Gas-Phase OH Radicals. *J. Phys. Chem. Lett.* **2015,** *6*, 527-534.
49. Lim, Y. B.; Ziemann, P. J. Effects of Molecular Structure on Aerosol Yields from OH Radical-Initiated Reactions of Linear, Branched, and Cyclic Alkanes in the Presence of NOx. *Environ. Sci. Technol.* **2009,** *43*, 2328-2334.

Table 1. The molecular structures and volatilities (saturation vapor pressure, v_p and the effective vapor pressure, c^*) of major reaction products formed in the heterogeneous OH oxidation of tartaric acid. The proposed hydrogen abstraction site is either on the tertiary carbon site (indicated by "-CH") or the hydroxyl group (indicated by "-OH").

Proposed compound (Chemical formula)	**Proposed molecular structure**	**Proposed hydrogen abstraction site**	**Molecular weight (g/mole)**	**v_p (atm)**	**c^* (μg m^{-3})**
2-hydroxy-3-oxosuccinic acid ($C_4H_4O_6$)	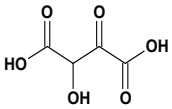	-CH	148.07	5.12×10^{-11}	3.15×10^{-1}
2-hydroxy-3-oxopropanoic acid ($C_3H_4O_4$)	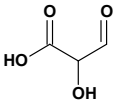	-OH	104.06	2.06×10^{-7}	8.90×10^{2}
Mesoxalic acid ($C_3H_2O_5$)	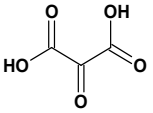	-CH	118.04	2.40×10^{-8}	1.18×10^{2}
2,3-dioxopropanoic acid ($C_3H_2O_4$)	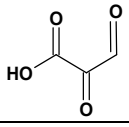	-OH	102.04	4.09×10^{-6}	1.73×10^{4}

	Tartaric acid	Succinic acid	2,3-dimethylsuccinic acid (2,3-DMSA)
Molecular formula	$C_4H_6O_6$	$C_4H_6O_4$	$C_6H_{10}O_4$
Oxidation state (OS_C)	1.5	0.5	-0.33

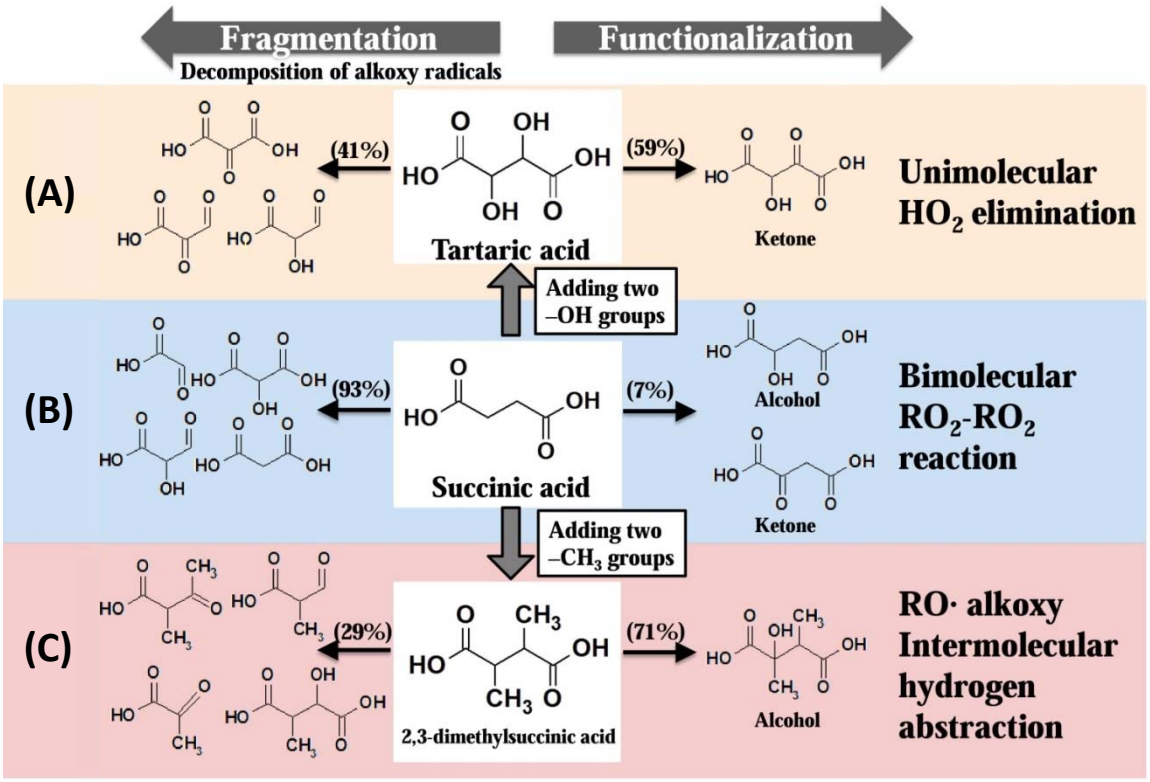

Figure 1. The molecular structure and proposed reaction mechanisms of 2,3-dimethylsuccinic acid, (**A**), succinic acid (**B**), and tartaric acid (**C**) during heterogeneous OH oxidation. Major functionalization and fragmentation products are shown. The percentage (%) listed indicates the abundance of total fragmentation and functionalization products at a similar OH exposure (~ 4×10^{11} molecule cm^{-3} s).

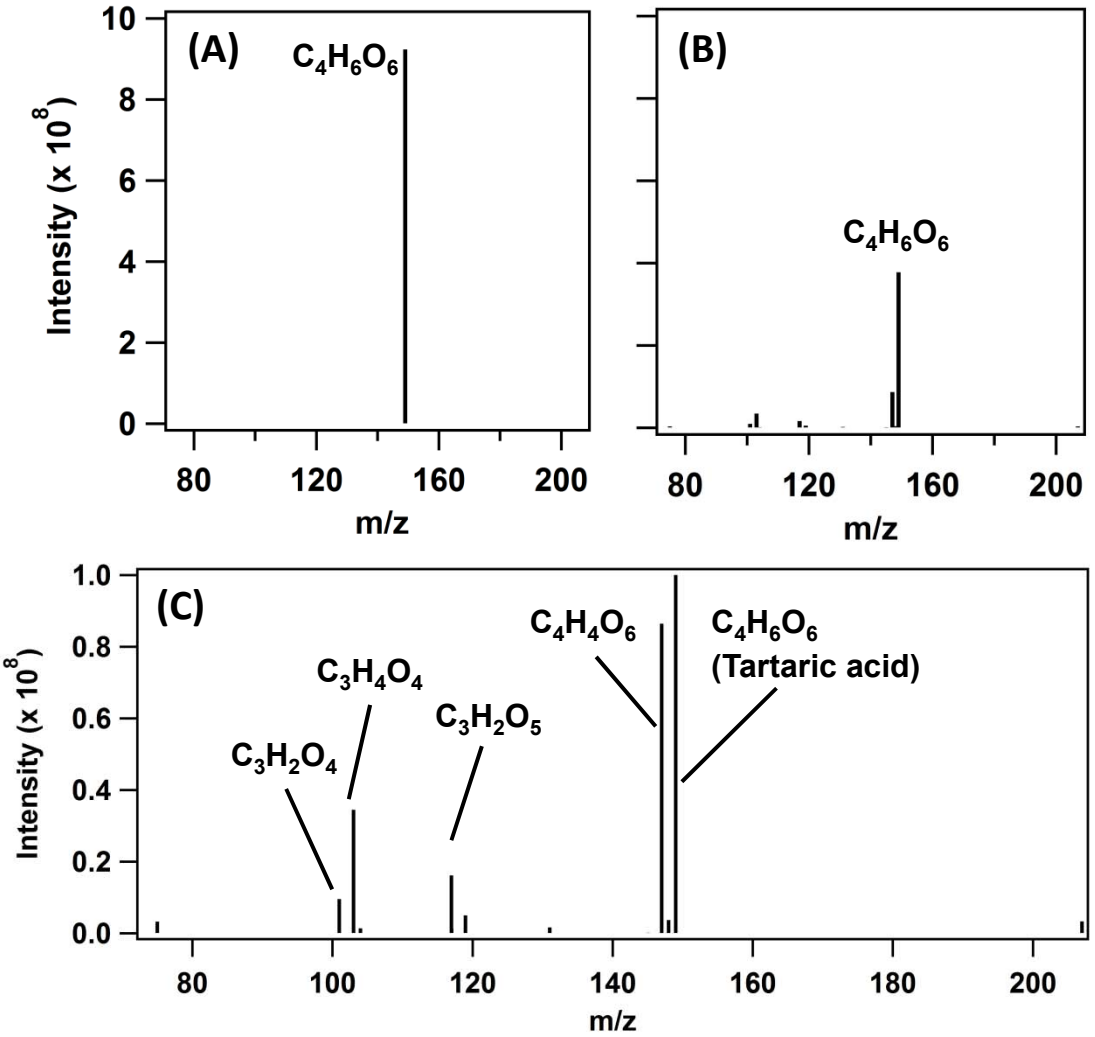

Figure 2 The aerosol mass spectra (**A**) before oxidation and (**B**) after oxidation (at OH exposure = 4.63×10^{11} molecule cm^{-3} s). A chemical formula is assigned for individual ion with an error of ±5ppm. The ion peaks for the major reaction products are shown in (**C**) over an enlarged scale. The unlabeled peaks contribute less than 1% of the total signal and have been detected in the background.

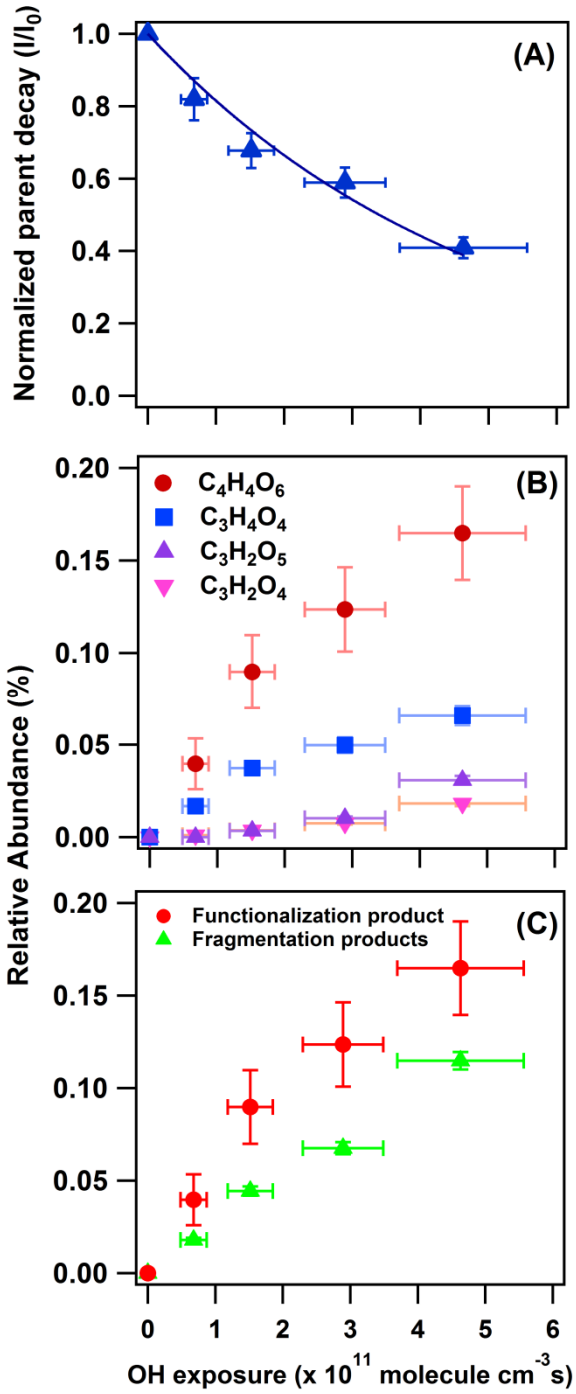

Figure 3. The heterogeneous OH oxidation of tartaric acid aerosols: (**A**) Normalized decay or tartaric acid, (**B**) Chemical evolution of the reaction products as a function of OH exposure; (**C**) The total relative abundance of the functionalization and fragmentation products. Error bars of one sigma are shown.

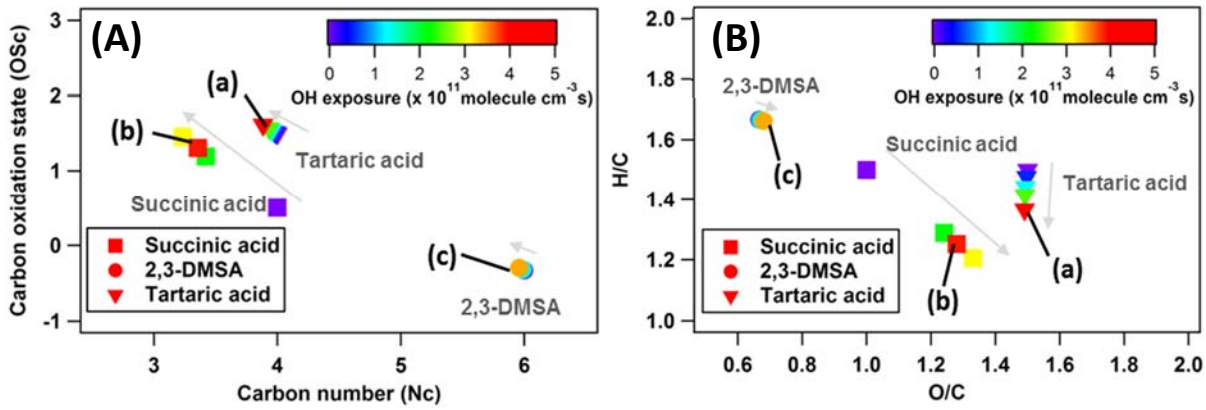

Figure 4. Chemical evolution in the aerosol composition for the heterogeneous OH oxidation of tartaric acid (triangle), 2,3-DMSA (circle), and succinic acid (square): (**A**) Carbon oxidation state (OS_C) versus carbon number (N_C) space ; (**B**) van Krevelen plot .

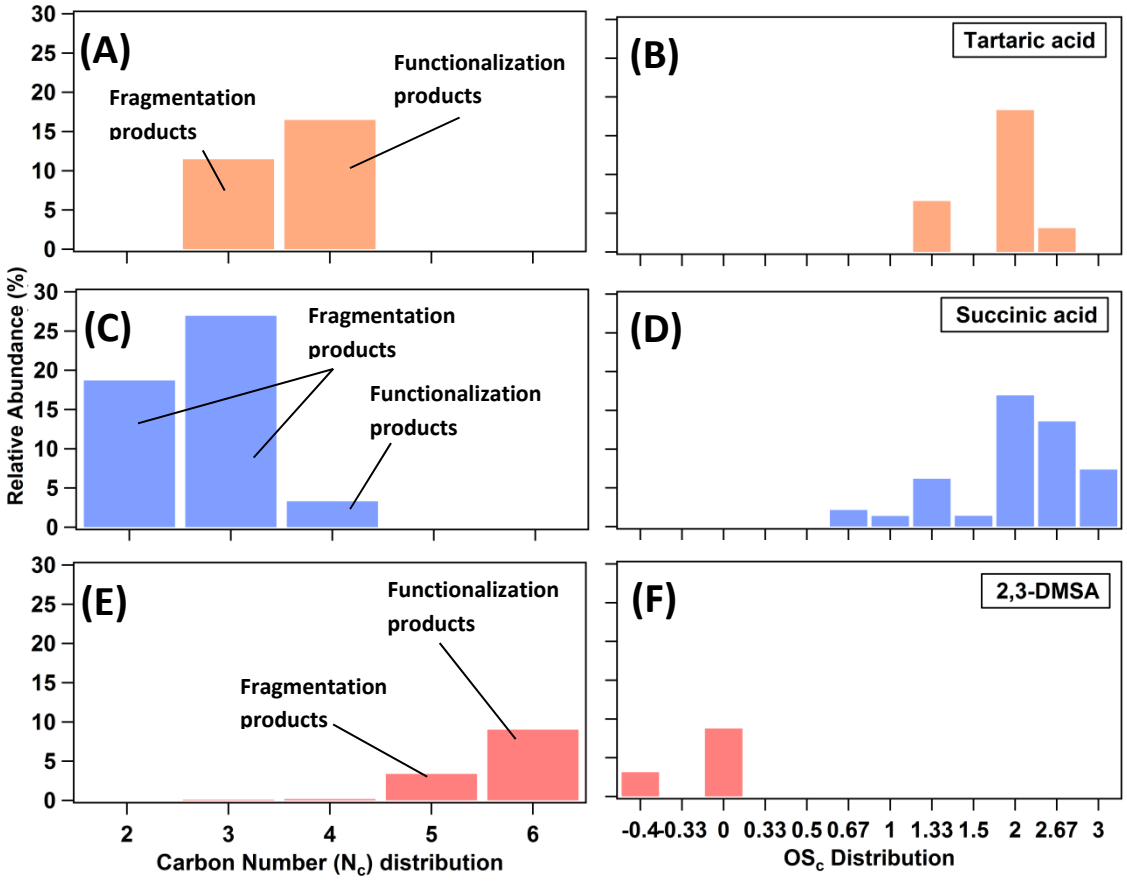

Figure 5. The distributions of molecular average carbon oxidation states (OS_C) and carbon number (N_C) for individual products at the points (a)-(c) marked in Figure 4. For the OS_C distribution data of 2,3-DMSA, only the major products are shown (the abundance of other minor individual products is less than 1%).

Scheme 1: Proposed reaction mechanisms for the heterogeneous OH oxidation of tartaric acid. The observed reaction products are shown in boxes. Major reaction pathways are highlighted in black and minor ones are shown in grey.

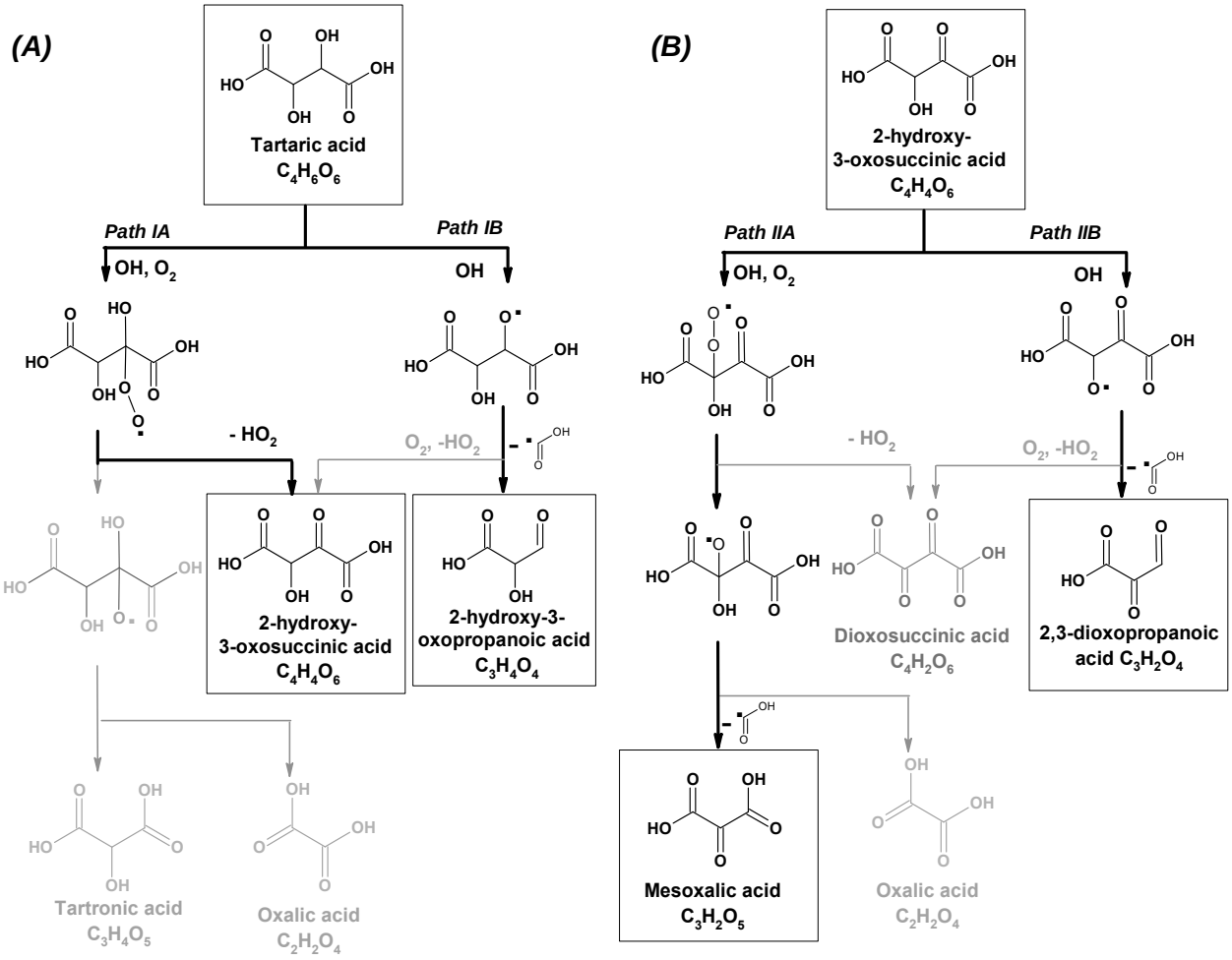

Scheme 2: Mechanism of the unimolecular HO_2 elimination process in an α-hydroxylperoxy radical.